SHCBP1 contributes to the proliferation and self-renewal of cervical cancer cells and activation of the NF-κB signaling pathway through EIF5A

BOYA DENG[1], AILIN LI[2], YING ZHU[1], YINGYING ZHOU[3], JING FEI[1] and YUAN MIAO[4]

[1]Department of Gynecology, The Second Affiliated Hospital of Zhejiang University, Hangzhou, Zhejiang 310009;
Departments of [2]Oncology and [3]Obstetrics and Gynecology, Shengjing Hospital of China Medical University,
Shenyang, Liaoning 110004; [4]Department of Pathology, The College of Basic Medicine Science and
The First Hospital of China Medical University, Shenyang, Liaoning 110001, P.R. China

Abstract. Cervical cancer (CC) is the most common human papillomavirus-related disease. Continuous activation of the NF-κB signaling pathway has been observed in CC. SHC binding and spindle associated 1 (SHCBP1) contributes to tumorigenesis and activation of the NF-κB pathway in multiple cancer types, while its function in CC remains unclear. In the present study, three Gene Expression Omnibus datasets were used to identify differentially expressed genes (DEGs) in CC. Loss- and gain-of-function experiments were performed using stable SHCBP1-silenced and SHCBP1-overexpressing CC cells. To further explore the molecular mechanism of SHCBP1 in CC, small interfering RNA targeting eukaryotic translation initiation factor 5A (EIF5A) was transfected into stable SHCBP1-overexpressing CC cells. The results demonstrated that SHCBP1 was an upregulated DEG in CC tissues compared with healthy control cervical tissues. Functional experiments revealed the pro-proliferative and pro-stemness role of SHCBP1 in CC cells (CaSki and SiHa cells), *in vitro*. Furthermore, the NF-κB signaling pathway in CC cells was activated by SHCBP1. Increases in cell proliferation, stemness and activation of NF-κB, induced by SHCBP1 overexpression in CC cells, were reversed by EIF5A knockdown. Taken together, the results indicated that SHCBP1 serves an important role in regulation of CC cell proliferation, self-renewal and activation of NF-κB via EIF5A. The present study demonstrated a potential molecular mechanism underlying the progression of CC.

Correspondence to: Dr Boya Deng, Department of Gynecology, The Second Affiliated Hospital of Zhejiang University, 88 Jiefang Road, Shangcheng, Hangzhou, Zhejiang 310009, P.R. China
E-mail: boyadeng@zju.edu.cn

Introduction

Cervical cancer (CC) is the fourth most common cancer and the fourth leading cause of cancer mortality in women (1). In 2020, 604,000 new diagnoses and 342,000 CC-related deaths were estimated worldwide, accounting for ~3.2% of all new cancer diagnoses and 3.4% of all cancer deaths (1). Given the high incidence and mortality of CC, the World Health Organization has assembled the CC Elimination Modelling Consortium to eliminate CC (2,3). Despite increases in human papillomavirus vaccination coverage, and advances in the screening approach of CC in recent years, the burden of CC is heavy in low-income countries (3). Therefore, it remains necessary to elucidate the molecular mechanisms underlying the progression of CC as it would help to identify effective therapeutic strategies.

The SHC binding and spindle associated 1 (SHCBP1) gene is located on chromosome 16q11.2; SHCBP1 is a member of the Src homolog and collagen homolog (Shc) family, and it was first characterized as a protein which bound to the Shc adaptor protein, Shc A (4). SHCBP1 is able to regulate cell proliferation, differentiation and wound inflammation (4,5). Increasing evidence has suggested that SHCBP1 is often dysregulated in cancer, and acts as a key regulator of tumor progression and metastasis in various types of cancer, such as gastric carcinoma (6), synovial sarcoma (7) and non-small cell lung carcinoma (8). Nevertheless, the functional and molecular mechanisms of SHCBP1 in CC remain unexplored.

As a transcription factor, NF-κB has been linked to inflammatory responses in various human diseases (9). In mammals, the NF-κB family is composed of five members, namely p65, c-Rel, RelB, p50 and p52, all of which share an N-terminal DNA-binding/dimerization domain referred to as the REL homology domain (10). NF-κB proteins form homo- and heterodimers that can bind to DNA sequences of target genes and ultimately regulate gene transcription (10). A strong association has been established between the activation of NF-κB and cancer, including CC (11-13). Zhou *et al* (14) confirmed the positive regulation of NF-κB signaling pathway activation and cell mobility in glioma induced by SHCBP1

by performing gain-/loss-of-function experiments. The link between SHCBP1 and NF-κB signaling in CC remains to be fully elucidated.

Eukaryotic translation initiation factor 5A (EIF5A), a key factor involved in translation elongation, exerts oncogenic roles in a variety of cancer types, including colorectal cancer (15), pancreatic cancer (16) and CC (17,18). EIF5A silencing has been reported to inhibit CC cell proliferation and promote NF-κB inhibitor (IκB) expression in CC cells (17). Furthermore, small interfering RNA (siRNA)-mediated inhibition of EIF5A has been shown to reverse the phosphorylation of p65 in multiple myeloma cells (19), highlighting the modulation of NF-κB activation by EIF5A. A dataset (GSE154307) downloaded from the Gene Expression Omnibus (GEO) database indicates that SHCBP1 short hairpin RNA (shRNA) reduced EIF5A mRNA expression in papillary thyroid cancer cells (20). Therefore, it was hypothesized that SHCBP1 may be involved in the activation of the NF-κB signaling pathway in CC cells via EIF5A.

In the present study, gain- and/or loss-of-function experiments were performed to explore the role of SHCBP1 in the proliferation and stemness of CC cells, and the *in vitro* activation of the NF-κB signaling pathway. In addition, the molecular mechanism of SHCBP1 in the progression of CC was discussed.

Materials and methods

Screening of differentially expressed genes (DEGs). The CC microarray datasets (GSE9750, GSE63514 and GSE7803) (21-23) were downloaded from the GEO database (https://www.ncbi.nlm.nih.gov/geo/). Genes with P<0.05 and log$_2$(fold change) ≥1 or ≤-1 were considered to be DEGs between healthy control cervical tissues and CC tissues.

Bioinformatics analysis. The Gene Expression Profiling Interactive Analysis (GEPIA, http://gepia.cancer-pku.cn/index.html) database was used to profile the expression level of SHCBP1 in tumor tissues from 31 types of cancer and the corresponding healthy control tissues based on the TCGA and GTEx databases. The mutual DEGs among the CC microarray datasets (GSE9750, GSE63514 and GSE7803) were identified using the online tool Venny 2.1 (https://bioinfogp.cnb.csic.es/tools/venny/index.html). The Database for Annotation, Visualization and Integrated Discovery (https://david.ncifcrf.gov/) was utilized to perform Gene Ontology (GO, http://geneontology.org/) and Kyoto Encyclopedia of Genes and Genomes (KEGG, https://www.genome.jp/kegg/) pathway enrichment analyses for the mutual DEGs.

Cell culture and transfection. Human CC cell lines were obtained from iCell Bioscience, Inc. (HeLa, cat. no. iCell-h088) and Procell Life Science & Technology Co., Ltd. (SiHa,C-33A and CaSki). HeLa, SiHa and C-33A cells were cultured in minimum essential medium (MEM, Beijing Solarbio Science & Technology Co., Ltd.) supplemented with 10% FBS (Zhejiang Tianhang Biotechnology Co., Ltd.), 100 U/ml penicillin and 0.1 mg/ml streptomycin with 5% CO$_2$ at 37°C. CaSki cells were maintained in RPMI-1640 medium (Beijing Solarbio Science & Technology Co., Ltd.) supplemented with 10% FBS (Zhejiang Tianhang Biotechnology Co., Ltd.),

100 U/ml penicillin and 0.1 mg/ml streptomycin with 5% CO$_2$ at 37°C.

For *in vitro* functional experiments, plasmids (2.5 μg) expressing shRNAs targeting SHCBP1 or non-targeting shRNAs (negative control, NC) were transfected into SiHa cells and plasmids (2.5 μg) expressing SHCBP1 coding DNA sequence (CDS) or empty vectors were transfected into CaSki cells using Lipofectamine® 3000 (Invitrogen; Thermo Fisher Scientific, Inc.) according to the manufacturer's instructions at 37°C, and the medium was changed after 8 h. The sequences of shRNAs were as follows: SHCBP1 shRNA-1, 5'-GGA TTGTATGTGTTTGGTTATTCAAGAGATAACCAAACA CATACAATCTTTTT-3'; SHCBP1 shRNA-2, 5'-GGGTTA TCAGAAGAATTCTATTCAAGAGATAGAATTCTTCTG ATAACCTTTTT-3'; and non-targeting shRNA, 5'-GTTCTC CGAACGTGTCACGTTTCAAGAGAACGTGACACGTTC GGAGAATTTTT-3'. The mock control represents the cells without any transfection. The shRNA was inserted into the pRNA-H1.1/Neo vector (cat. no. SD1203; GenScript) between *Bam*HI and *Hin*dIII. The SHCBP1 CDS (General Biology (Anhui) Co., Ltd.) was inserted into the pcDNA3.1(+) vector (cat. no. V79020; Invitrogen; Thermo Fisher Scientific, Inc.) between *Hin*dIII and *Xho*I. At 24 h post-transfection, the SiHa cells stably silencing SHCBP1 were selected in complete MEM containing 350 μg/ml geneticin (Beijing Solarbio Science & Technology Co., Ltd.) for 1-2 weeks, and the CaSki cells stably overexpressing SHCBP1 were selected in complete RPMI-1640 medium containing 300 μg/ml geneticin for 1-2 weeks, and the medium was changed every 2-3 days. A large number of cells died after 1- or 2-week geneticin selection, and then the surviving cells were cultured in complete MEM or RPMI-1640 medium containing geneticin (SiHa: 175 μg/ml; CaSki: 150 μg/ml) for 2 weeks.

In addition, stable SHCBP1-overexpressing CaSki cells or blank CaSki cells (without any manipulation of SHCBP1 expression) were transfected with siRNA-targeting EIF5A (75 pmol; General Biology (Anhui) Co., Ltd.) using Lipofectamine® 3000 (Invitrogen; Thermo Fisher Scientific, Inc.) at 37°C, and the medium was changed after 8 h. The sequences of siRNAs were as follows: EIF5A siRNA sense, 5'-GCAAGGAGAUUG AGCAGAATT-3' and anti-sense 5'-UUCUGCUCAAUCUCC UUGCTT-3'; and non-targeting siRNA sense, 5'-UUCUCC GAACGUGUCACGUTT-3' and anti-sense, 5'-ACGUGACAC GUUCGGAGAATT-3'. At 48 h post-transfection, the cells were used for subsequent experiments.

RNA extraction and reverse transcription-quantitative PCR (RT-qPCR). Total RNA was extracted from the four CC cell lines with TRIpure reagent (BioTeke Corporation). First-strand cDNA was synthesized using BeyoRT II M-MLV reverse transcriptase (Beyotime Institute of Biotechnology) with dNTPs, 5x buffer, Rnase inhibitor (BioTeke Corporation), oligo (dT)$_{15}$ and random primers at 25°C for 10 min, at 42°C for 50 min and at 80°C for 10 min. Relative mRNA expression was determined by RT-qPCR on an Exicycler™ 96 Real-Time PCR system (Bioneer Corporation) using SYBR Green 2x Taq PCR Master Mix (Beijing Solarbio Science & Technology Co., Ltd.) and gene-specific primers (General Biology (Anhui) Co., Ltd.). The thermocycling conditions were listed as follows: 94°C for 5 min (initial denaturation), 40 cycles of 94°C for 10 sec, 60°C

for 20 sec and 72˚C for 30 sec, followed by a single final extension for 2.5 min at 72˚C. GAPDH was used to normalize gene expression. The relative expression levels of mRNAs were calculated using the $2^{-\Delta\Delta Cq}$ method (24). The sequences of the gene-specific primers used in RT-qPCR are listed in Table I.

Western blotting. Protein was extracted from the four CC cell lines with RIPA buffer (Beijing Solarbio Science & Technology Co., Ltd.) containing 1 mM phenylmethanesulfonyl fluoride (Beijing Solarbio Science & Technology Co., Ltd.). The concentration of protein was measured using BCA protein assay kits (Beijing Solarbio Science & Technology Co., Ltd.) according to the manufacturer's protocols. Protein samples (10-20 µg/lane) were separated by SDS-PAGE on 10 or 14% gels and transferred to PVDF membranes (MilliporeSigma). The membranes were blocked with 5% BSA (Biosharp Life Sciences) at room temperature for 1 h, followed by incubation with anti-SHCBP1 (dilution, 1:500; cat no. 12672-1-AP, Proteintech Group, Inc.), anti-cyclin D1 (dilution, 1:500; cat no. A19038, ABclonal Biotech Co., Ltd.), anti-p21 (dilution, 1:500; cat no. A19094, ABclonal Biotech Co., Ltd.), anti-phosphorylated (p)-IκBα (dilution, 1:500; Ser-32/Ser-36, cat no. AF2002, Affinity Biosciences, Ltd.), anti-IκBα (dilution, 1:1,000; cat no. AF5002, Affinity Biosciences, Ltd.), anti-p-p65 (dilution, 1:400; Ser-536, cat no. AF2006, Affinity Biosciences, Ltd.), anti-p65 (dilution, 1:1,000; cat no. AF5006, Affinity Biosciences, Ltd.), anti-EIF5A (dilution, 1:1,000; cat no. 11309-1-AP, Proteintech Group, Inc.), and anti-GAPDH (dilution, 1:10,000; cat no. 60004-1-Ig, Proteintech Group, Inc.) antibodies overnight at 4˚C. The following day, membranes were incubated with HRP-conjugated goat anti-rabbit IgG (dilution, 1:3,000; cat no. SE134, Beijing Solarbio Science & Technology Co., Ltd.) or goat anti-mouse IgG (dilution, 1:3,000; cat no. SE131, Beijing Solarbio Science & Technology Co., Ltd.) for 1 h at 37˚C. The immunoreactive protein bands were visualized using an ECL kit (Beijing Solarbio Science & Technology Co., Ltd.). GAPDH was used as a loading control to normalize protein expression.

Cell proliferation assays. MTT assays were used to assess cell proliferation. In brief, CC cells were seeded into 96-well culture plates at a density of $4x10^3$ cells/well and cultured for 0, 12, 24, 36 and 48 h. Cell proliferation was measured using MTT assay kits (Nanjing KeyGen Biotech Co., Ltd.) according to the manufacturer's instructions. DMSO (Nanjing KeyGen Biotech Co., Ltd.) was used to dissolve formazan and the optical density was measured at 490 nm.

Immunofluorescence assays (IFAs). SiHa and CaSki cells were grown on glass coverslips ($1x10^5$ cells per well) in 24-well plates, fixed in 4% paraformaldehyde (Sinopharm Chemical Reagent Co., Ltd.) for 15 min at room temperature and permeabilized with 0.1% Triton X-100 (Beyotime Institute of Biotechnology) for 30 min at room temperature. After blocking with 1% BSA (Sangon Biotech Co., Ltd.) for 15 min at room temperature, the coverslips were incubated with anti-ki67 (dilution, 1:200; cat no. A11390, ABclonal Biotech Co., Ltd.) or anti-p65 antibodies (dilution, 1:200; cat no. A19653, ABclonal Biotech Co., Ltd.) at 4˚C overnight, followed by incubation with the Alexa Fluor™ 555-conjugated goat anti-rabbit (dilution, 1:200;

Table I. Sequences of primers used in reverse transcription-quantitative PCR analysis.

Gene	Sequences (5'-3')
Human SHCBP1	Forward: ATCCAAGCAAAGGGTGTC
	Reverse: CAAAGCCTGTCCGTAAGC
Human EIF5A	Forward: TAAGAATGGCTTTGTGGTG
	Reverse: TGTCCTGGAGCAGTGATAG
Human CD133	Forward: GCACTCTATACCAAAGCGT CAA
	Reverse: CTCCCATACTTCTTAGTTTC CTCA
Human CD44	Forward: ATCCCTGCTACCACTTTG
	Reverse: TTCTTCATTTGGCTCCC
Human NANOG	Forward: CACCTATGCCTGTGATTT
	Reverse: CAGAAGTGGGTTGTTTGC
Human OCT4	Forward: GTGGAGGAAGCTGACAAC AATG
	Reverse: CTCACTCGGTTCTCGATAC TGG
Human GAPDH	Forward: GACCTGACCTGCCGTCTAG
	Reverse: AGGAGTGGGTGTCGCTGT

EIF5A, eukaryotic translation initiation factor 5A; SHCBP1, SHC binding and spindle associated 1.

cat no. A27039, Invitrogen; Thermo Fisher Scientific, Inc.) at room temperature for 1 h. Cell nuclei were stained with DAPI (Shanghai Aladdin Biochemical Technology Co., Ltd.) at room temperature for 5 min and observed under a fluorescence microscope. Total p65 and nuclear p65 levels were quantified. Relative p65 nuclear localization was expressed as the ratio of the fluorescence density of nuclear p65 staining to the fluorescence density of total p65 cellular staining.

Cell cycle analysis. Cell cycle progression was examined using cell cycle analysis kits (cat no. BL114A, Biosharp Life Sciences). SiHa and CaSki cells ($5x10^5$ cells) were collected by centrifugation (106 x g for 5 min) at 4˚C and fixed with ice-cold 70% ethanol for 2 h at 4˚C. The cell pellets were washed with PBS twice and the staining buffer, PI (20x) and RNase A (50x) (cat no. BL114A, Biosharp Life Sciences) were added. After incubation at 37˚C for 30 min, the cells were analyzed by a flow cytometer (NovoCyte 2040R; ACEA Bioscience, Inc.; Agilent Technologies, Inc.) using the NovoExpress software (version 1.4.1; ACEA Bioscience, Inc.; Agilent Technologies, Inc.).

Sphere formation assays. CC cells were seeded into 6-well ultra-low plates at a density of $3x10^3$ cells/ml and cultured in stem cell medium for 2 weeks with 5% CO_2 at 37˚C. The medium was changed every 2 days. The stem cell medium was DMEM/F12 (Procell Life Science & Technology Co., Ltd.) supplemented with 1% B-27 (Gibco; Thermo Fisher Scientific, Inc.), 1% N-2 (Gibco; Thermo Fisher Scientific, Inc.), 20 ng/ml EGF (Sino Biological Inc.) and 10 ng/ml FGF (Sino Biological Inc.). Spheres were observed
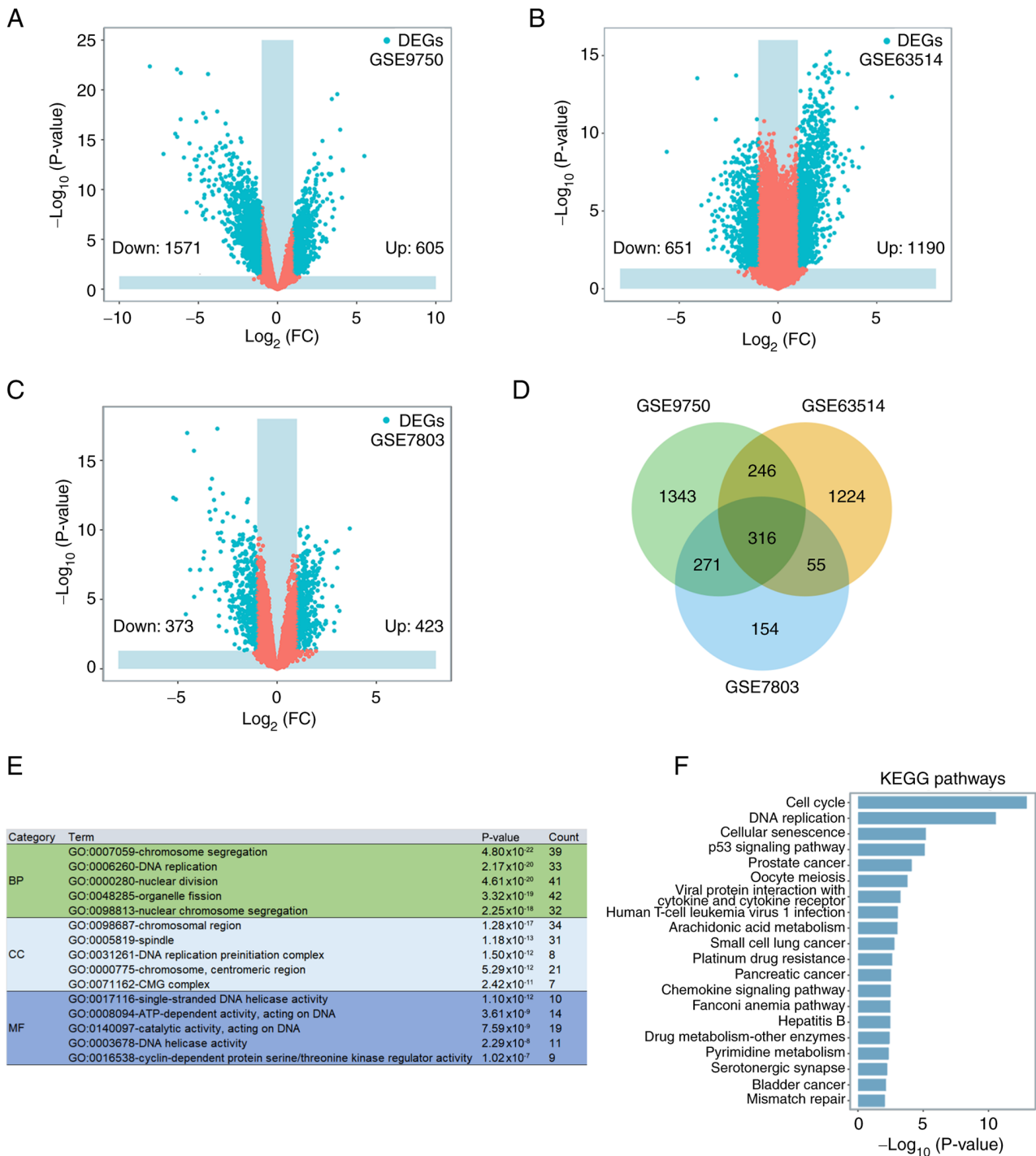
Figure 1. Identification of DEGs in cervical cancer. Volcano plots illustrating DEGs in the microarray datasets (A) GSE9750, (B) GSE63514 and (C) GSE7803. (D) Venn diagram of DEGs among the three datasets. (E) GO analysis of the mutual DEGs. (F) KEGG pathway analysis of the mutual DEGs. BP, biological process; CC, cell component; DEGs, differentially expressed genes; FC, fold change; GO, Gene Ontology; KEGG, Kyoto Encyclopedia of Genes and Genomes; MF, molecular function.

under an inverted phase contrast microscope and analyzed using Image-Pro Plus software (version 6.0, Media Cybernetics, Inc.). Spherical cell clusters were considered to be spheres when their diameter was >75 μm. The spheres were formed based on the cancer stem cell (CSC)-like properties of cancer cells.

Statistical analysis. Statistical analysis was performed using GraphPad Prism (version 8.0.2, GraphPad Software; Dotmatics). Results are presented as the mean ± SD from three independent experiments. One-way and two-way ANOVA followed by Tukey or Sidak tests, unpaired t-test and Mann Whitney U test were used to analyze statistical significance. $P<0.05$ was considered to indicate a statistically significant difference.

Results

Identification of DEGs in CC. The GSE9750, GSE63514 and GSE7803 datasets indicated 2,176, 1,841 and 796 DEGs in CC
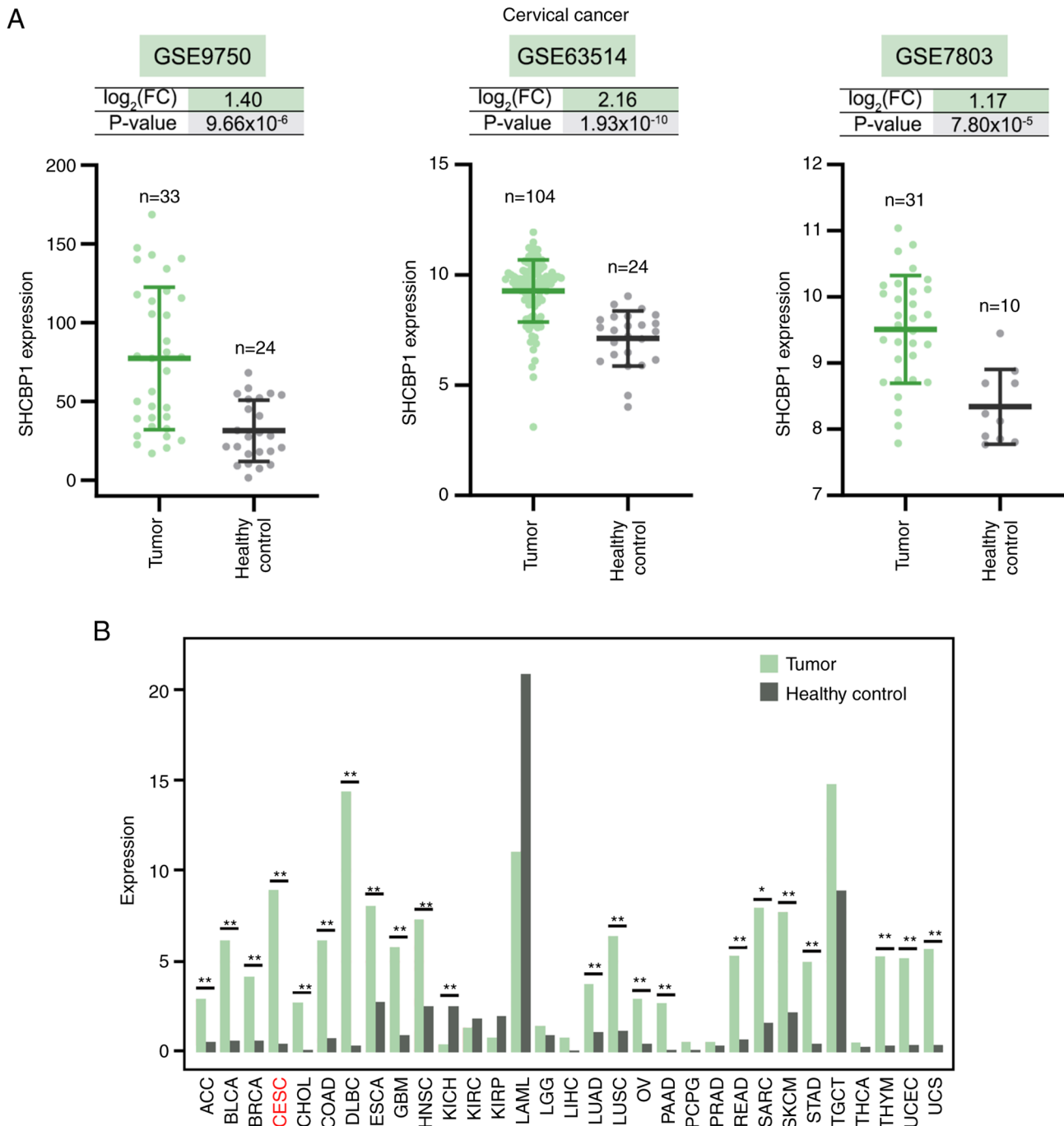
Figure 2. SHCBP1 expression in cervical cancer and other cancer types. (A) SHCBP1 expression in the GSE9750, GSE63514 and GSE7803 datasets downloaded from the Gene Expression Omnibus database. (B) Pan-cancer expression profiling analysis of SHCBP1 using the Gene Expression Profiling Interactive Analysis database. *P<0.05 and **P<0.01. SHCBP1, SHC binding and spindle associated 1; FC, fold change; ACC, adrenocortical carcinoma; BLCA, bladder urothelial carcinoma; BRCA, breast invasive carcinoma; CESC, cervical squamous cell carcinoma and endocervical adenocarcinoma; CHOL, cholangiocarcinoma; COAD, colon adenocarcinoma; DLBC, lymphoid neoplasm diffuse large B-cell lymphoma; ESCA, esophageal carcinoma; GBM, glioblastoma multiforme; HNSC, head and neck squamous cell carcinoma; KICH, kidney chromophobe; KIRC, kidney renal clear cell carcinoma; KIRP, kidney renal papillary cell carcinoma; LAML, acute myeloid leukemia; LGG, brain lower grade glioma; LIHC, liver hepatocellular carcinoma; LUAD, lung adenocarcinoma; LUSC, lung squamous cell carcinoma; OV, ovarian serous cystadenocarcinoma; PAAD, pancreatic adenocarcinoma; PCPG, pheochromocytoma and paraganglioma; PRAD, prostate adenocarcinoma; READ, rectum adenocarcinoma; SARC, sarcoma; SKCM, skin cutaneous melanoma; STAD, stomach adenocarcinoma; TGCT, testicular germ cell tumors; THCA, thyroid carcinoma; THYM, thymoma; UCEC, uterine corpus endometrial carcinoma; UCS, uterine carcinosarcoma.

compared with the healthy control cervical tissues, respectively (Fig. 1A-C). The Venn diagram of DEGs in the three datasets indicated a total of 316 mutual DEGs (Fig. 1D). The function of the mutual DEGs was examined by performing GO (Fig. 1E) and KEGG pathway (Fig. 1F) enrichment analyses.

GO analysis suggested that the mutual DEGs were mainly linked to 'chromosome segregation' [biological process (BP)], 'DNA replication' (BP), 'nuclear division' (BP), 'chromosomal region' [cell component (CC)], 'spindle' (CC), 'DNA replication preinitiation complex' (CC), 'single-stranded DNA
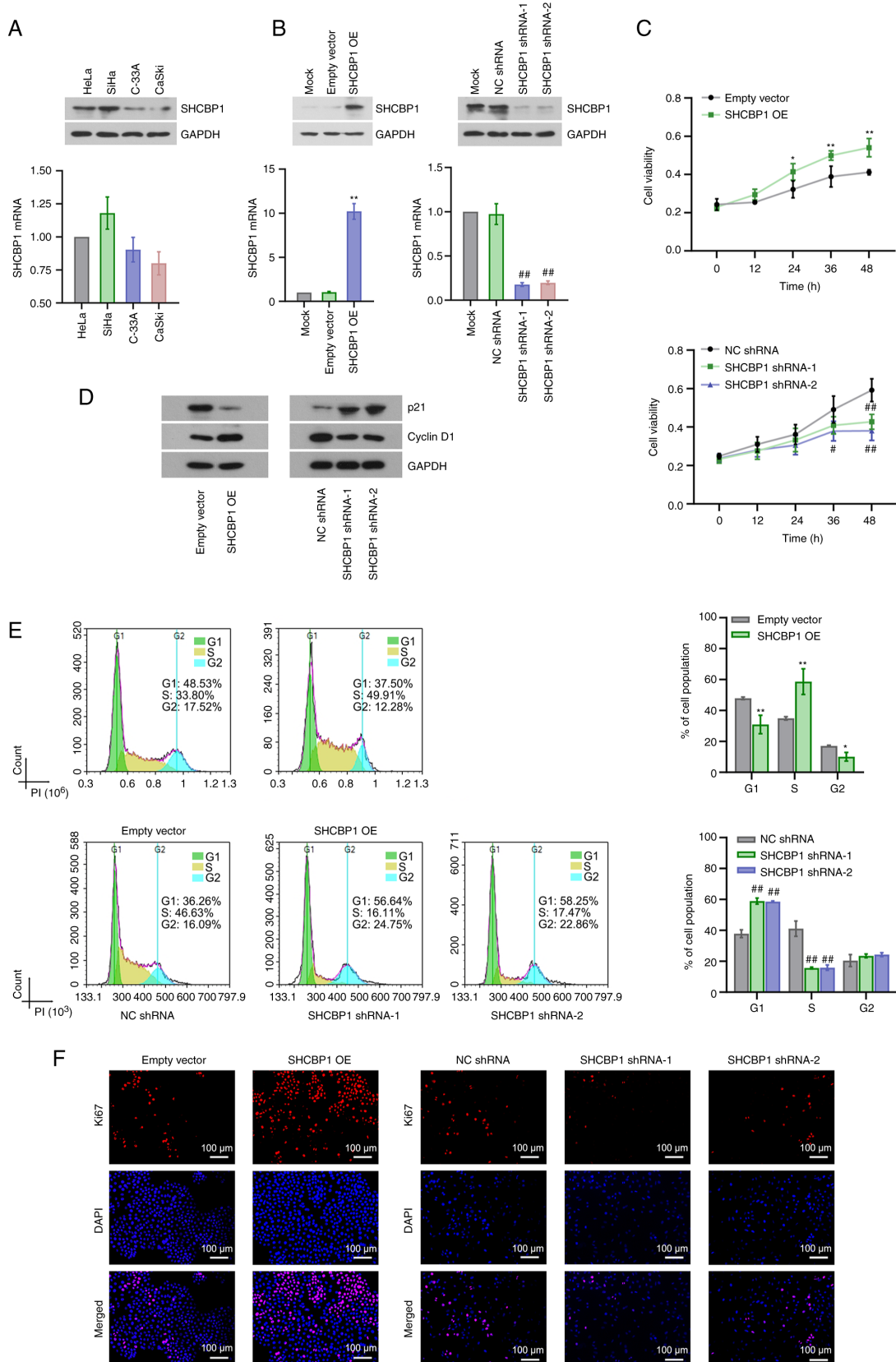
Figure 3. Effect of SHCBP1 on the proliferation of CC cells. (A) SHCBP1 mRNA and protein expression in the HeLa, SiHa, C-33A and CaSki CC cell lines. Relatively high and low SHCBP1 expression was observed in SiHa and CaSki cells compared with that in HeLa cells, respectively. (B) Stable knockdown and overexpression of SHCBP1 in SiHa and CaSki cells. SHCBP1 mRNA and protein expression of stable SHCBP1-overexpressing and SHCBP1-silenced CC cell lines was measured by reverse transcription-quantitative PCR and western blotting. Data were analyzed with one-way ANOVA followed by Tukey tests. (C) Cell proliferation was measured using an MTT assay. Data were analyzed with two-way ANOVA followed by Sidak or Tukey tests. (D) Western blot analysis of p21 and cyclin D1. (E) Flow cytometric analysis of cell cycle distribution. Data were analyzed with unpaired t-test or one-way ANOVA followed by Tukey tests (F) Ki67 expression was detected by immunofluorescence assays. Scale bar, 100 μm. Data are presented as the mean ± SD. *P<0.05 and **P<0.01 vs. empty vector group. #P<0.05 and ##P<0.01 vs. NC shRNA group. n=3. CC, cervical cancer; NC, negative control; OE, overexpression; SHCBP1, SHC binding and spindle associated 1; shRNA, short hairpin RNA.
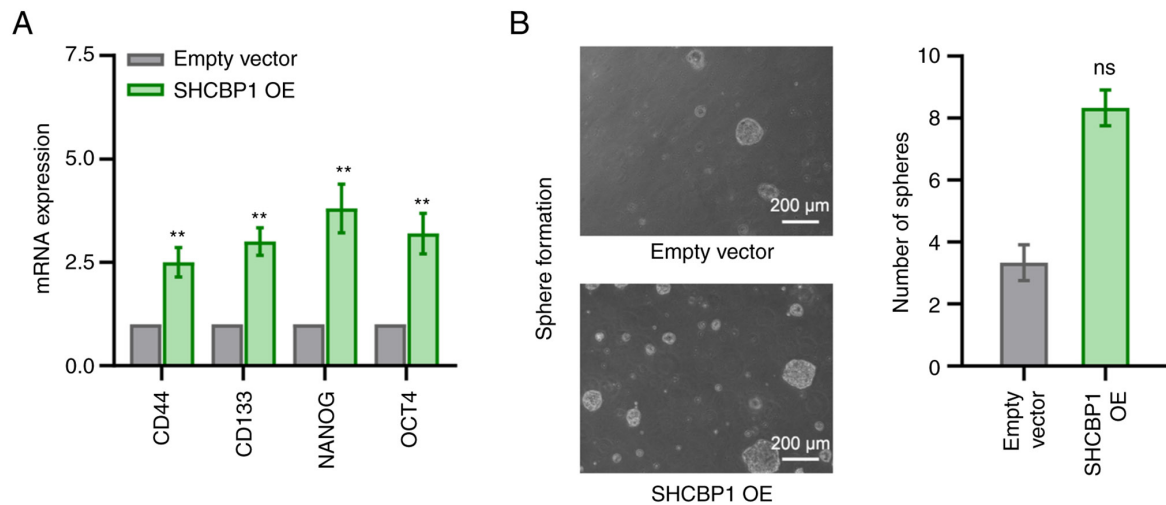
Figure 4. Effect of SHCBP1 on the stemness of CC cells. (A) mRNA expression levels of CD44, CD133, NANOG and OCT4 in the stable SHCBP1-overexpressing CaSki cell lines was measured by reverse transcription-quantitative PCR. Data were analyzed with unpaired t-test. (B) Sphere formation ability of the stable SHCBP1-overexpressing CC cell lines. Scale bar, 200 μm. Data were analyzed using the Mann Whitney U test. Data are presented as the mean ± SD. **P<0.01 vs. empty vector group. n=3. CC, cervical cancer; ns, no significance; OE, overexpression; SHCBP1, SHC binding and spindle associated 1.

helicase activity' [molecular function (MF)], 'ATP-dependent activity, acting on DNA' (MF) and 'catalytic activity, acting on DNA' (MF). The three most enriched pathways in the KEGG analysis were 'cell cycle', 'DNA replication' and 'cellular senescence'.

Upregulation of SHCBP1 mRNA levels in CC. The mRNA expression level of SHCBP1 was upregulated in CC compared with the healthy control cervix tissues in the GSE9750, GSE63514 and GSE7803 datasets, and the expression of SHCBP1 in the tumor and healthy control cervical tissues in the three datasets was shown in Fig. 2A. The Gene Expression Profiling Interactive Analysis database showed that SHCBP1 expression was significantly upregulated in 21 human cancer types, particularly lymphoid neoplasm diffuse large B-cell lymphoma and cervical squamous cell carcinoma and endocervical adenocarcinoma (Fig. 2B). The highest median value of SHCBP1 expression was observed in the healthy control for acute myeloid leukemia, which indicated a high level of SHCBP1 mRNA in bone marrow (Fig. 2B). There was not a statistically significant difference between the bone marrow from the healthy control and acute myeloid leukemia patients (Fig. 2B).

Pro-proliferative and pro-stemness role of SHCBP1 in CC cells in vitro. The basal expression levels of SHCBP1 in HeLa, SiHa, C-33A and CaSki CC cell lines were determined by RT-qPCR and western blotting and the results demonstrated a markedly higher expression of SHCBP1 in SiHa cells and a markedly lower expression of SHCBP1 in CaSki cells than that in other CC cell lines (Fig. 3A). Stable SHCBP1-overexpressing CaSki cells and stable SHCBP1-silenced SiHa cells were successfully established (Fig. 3B). MTT assays demonstrated that SHCBP1 overexpression promoted but SHCBP1 knockdown inhibited cell proliferation *in vitro* (Fig. 3C). Proteins involved in cell cycle progression were detected by western blotting. SHCBP1 overexpression promoted cyclin D1 expression and inhibited p21

expression in CaSki cells, yet SHCBP1 knockdown induced an opposite effect on SiHa cells (Fig. 3D). Flow cytometric analysis suggested that SHCBP1 overexpression enhanced entry into the S phase but SHCBP1 knockdown induced arrest at the G1 phase of the cell cycle (Fig. 3E). In addition, SHCBP1 overexpression decreased the number of cells at the G2 phase, which might be the result of the extreme increases in cell density induced by SHCBP1 overexpression (Fig. 3E). IFA of ki67 showed increased ki67 expression induced by SHCBP1 overexpression and decreased ki67 expression induced by SHCBP1 knockdown, which indicated the pro-proliferative roles of SHCBP1 (Fig. 3F). Subsequently, the effect of SHCBP1 on the CSC-like properties of CC cells was investigated. The mRNA expression levels of stemness-related markers, including CD44, CD133, NANOG and OCT4, were analyzed, and the results demonstrated that SHCBP1 overexpression significantly increased the mRNA expression levels of these markers (Fig. 4A). Furthermore, SHCBP1 overexpression tended to upregulate the sphere-forming ability of CC cells, although there was no statistically significant difference between the empty vector and the SHCBP1 OE group (Fig. 4B). Taken together, SHCBP1 exerted a key role in maintaining the malignant phenotype and self-renewal of CC cells *in vitro*.

Activation of the NF-κB signaling pathway by SHCBP1 in CC cells. Activation of the NF-κB pathway serves a key role in cancer (25). The phosphorylation of IκBα and p65 was assessed by western blotting. SHCBP1 overexpression increased p-IκBα (Ser-32/Ser-36) and p-p65 (Ser-536) expressions but decreased total IκBα expression, however, SHCBP1 knockdown exerted the opposite effect (Fig. 5A). IFA for p65 demonstrated that a significantly higher number of positive signals of p65 was detected in the nucleus after SHCBP1 overexpression; however, SHCBP1 knockdown significantly reduced nuclear signals of p65 (Fig. 5B). These findings suggested that SHCBP1 was involved in the activation of the NF-κB signaling pathway in CC cells.
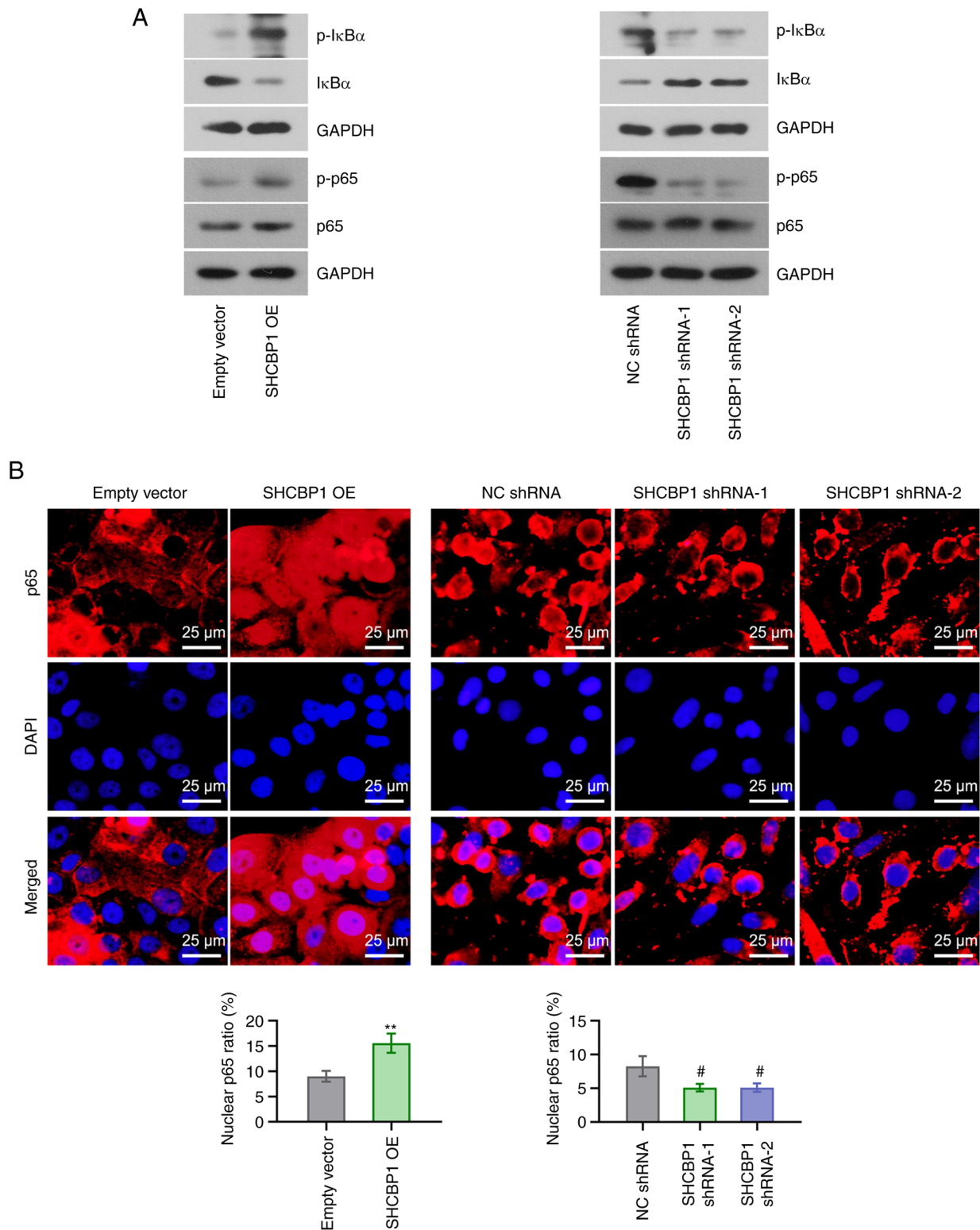
Figure 5. Effect of SHCBP1 on the activation of p65 in cervical cancer cells. (A) Protein expression levels of p-IκBα, IκBα, p-p65 and p65 were determined by western blotting and GAPDH was used as a loading control. (B) Immunofluorescence assay for p65. Scale bar, 25 µm. The ratio for nuclear p65 was quantified. Data were analyzed with unpaired t-test or one-way ANOVA followed by Tukey's test. Data are presented as the mean ± SD. **P<0.01 vs. empty vector group. #P<0.05 vs. NC shRNA group. n=3. IκBα, NF-κB inhibitor α; NC, negative control; OE, overexpression; p-, phosphorylated; SHCBP1, SHC binding and spindle associated 1; shRNA, short hairpin RNA.

SHCBP1 depends on EIF5A to exert pro-proliferative and self-renewal effects and activate the NF-κB signaling pathway in CC cells. EIF5A exerts oncogenic roles in CC (17,18). A GEO dataset (GSE154307) indicates downregulated EIF5A mRNA expression by SHCBP1 shRNA in papillary thyroid cancer cells (20). The results of the present study demonstrated that EIF5A mRNA expression was significantly promoted by SHCBP1 overexpression (Fig. S1A), yet significantly inhibited
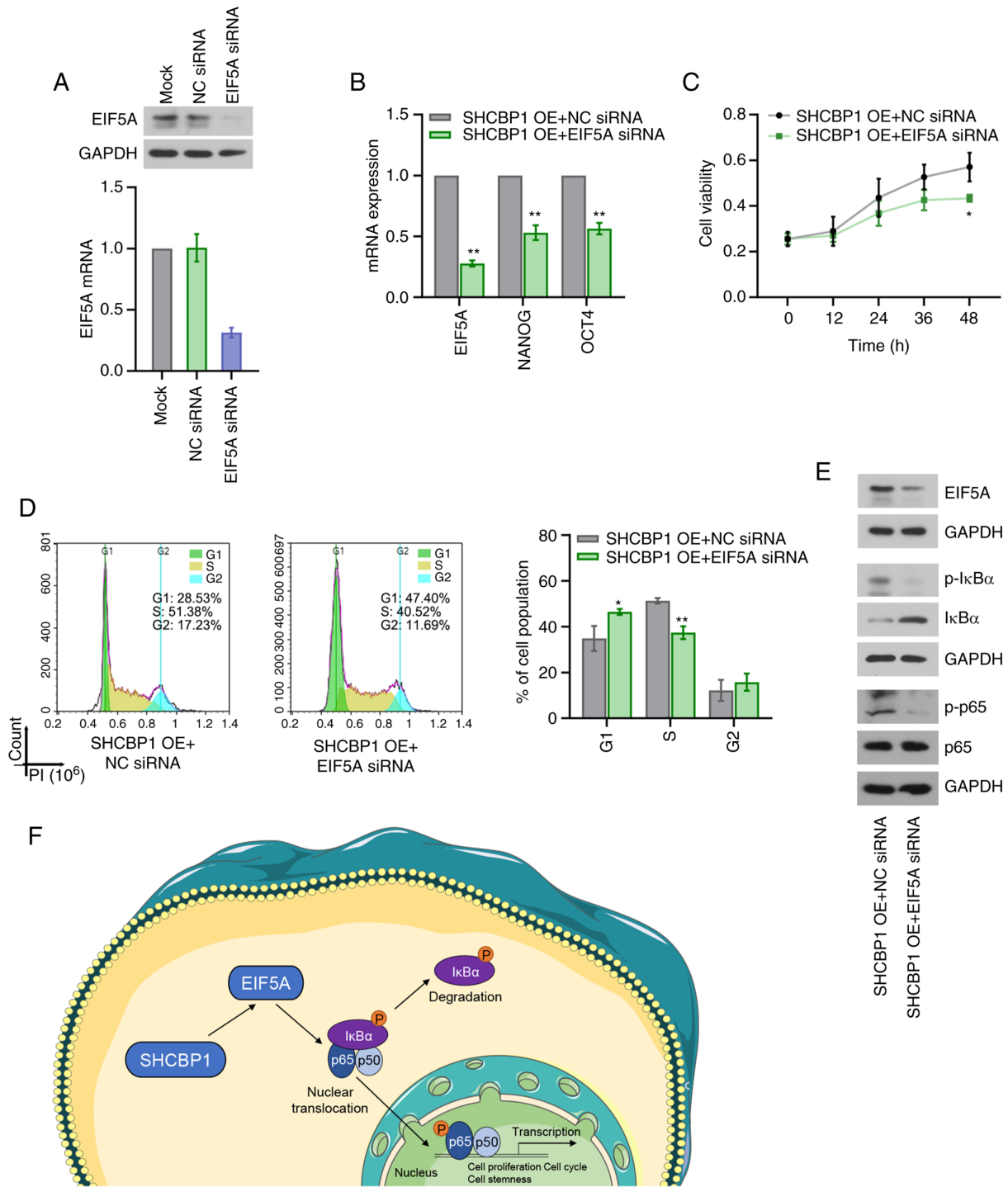
Figure 6. Effect of EIF5A on cell proliferation, cell stemness and activation of the NF-κB signaling pathway induced by SHCBP1 in CC. CaSki cells were transiently transfected with EIF5A siRNA. (A) Knockdown efficiency was evaluated by measuring mRNA and protein expression levels of EIF5A using RT-qPCR and western blotting. Data were analyzed with one-way ANOVA followed by Tukey's test. **P<0.01 vs. NC siRNA group. (B) CaSki cells stably overexpressing SHCBP1 were transiently transfected with EIF5A siRNA. The mRNA expression levels of EIF5A, NANOG and OCT4 were examined by RT-qPCR. Data were analyzed with unpaired t-test. (C) Cell proliferation was measured using an MTT assay. Data were analyzed with two-way ANOVA followed by Sidak's test. (D) Flow cytometric analysis of cell cycle distribution. Data were analyzed with unpaired t-test. (E) Western blot analysis of EIF5A, p-IκBα, IκBα, p-p65 and p65. (F) Schematic overview of the molecular mechanism underlying the function of SHCBP1 in CC cells. Data are presented as the mean ± SD. *P<0.05 and **P<0.01 vs. SHCBP1-OE + NC siRNA group. n=3. CC, cervical cancer; EIF5A, eukaryotic translation initiation factor 5A; IκBα, NF-κB inhibitor α; NC, negative control; OE, overexpression; p-, phosphorylated; RT-qPCR, reverse transcription-quantitative PCR; SHCBP1, SHC binding and spindle associated 1; siRNA, small interfering RNA.

by SHCBP1 knockdown (Fig. S1B). To investigate whether EIF5A mediated the biological function of SHCBP1 in CC cells, untransfected CaSki cells and stable SHCBP1-overexpressing CaSki cells were transiently transfected with EIF5A siRNA.

The knockdown efficiency of EIF5A was verified in untransfected CaSki cells and stable SHCBP1-overexpressing CaSki cells by RT-qPCR and western blotting (Fig. 6A, B and E). The stemness-related markers including NANOG and OCT4 were

confirmed to be regulated by EIF5A (26). EIF5A siRNA inhibited the SHCBP1-induced increases in NANOG and OCT4 expression (Fig. 6B). In addition, EIF5A siRNA reversed the pro-proliferative effects (Fig. 6C, D) and the activation of the NF-κB signaling pathway induced by SHCBP1 overexpression (Fig. 6E). These results confirmed that SHCBP1 enhanced the malignant phenotype and self-renewal of CC cells, and activated the NF-κB signaling pathway *in vitro* via EIF5A. The potential mechanism of SHCBP1 in CC cells is shown in Fig. 6F. Based on the findings of the present study, it was hypothesized that SHCBP1 increased the nuclear translocation of p65 via EIF5A, thereby enhancing the NF-κB-mediated gene transcription and promoting cell proliferation and cell stemness.

Discussion

Unchecked proliferation is a fundamental hallmark of cancer cells (27). The accurate transition from the G1 phase to the S phase of the cell cycle is crucial for the control of cell proliferation, and its disorganization results in uncontrolled cell proliferation (28). SHCBP1 was first identified in proliferating cells and it was absent in quiescent tissues and growth-arrested cells (4). SHCBP1 mRNA is expressed during entry into S phase and its expression was higher in cells treated with a stimulator of cell cycle progression (4). These evidence indicate the important role of SHCBP1 in regulating cell proliferation and cell cycle progression (4). The present study revealed that SHCBP1 increased CC cell proliferation, ki67 expression and cell cycle transition from the G1 phase to the S phase of the cell cycle. The pro-proliferative effect of SHCBP1 has also been observed in cell lines from other types of cancer (20,29-32), highlighting the important role of SHCBP1 in cancer cell proliferation. Therefore, SHCBP1 inhibition may be a potential strategy for the control of tumor progression.

CSCs, a key population of tumor cells, are pluripotent, self-renewing and they contribute to tumor initiation, metastasis, recurrence and resistance to therapies (33). Cumulative reports have highlighted the importance of CSCs in CC (34-36). SHCBP1 knockdown induced inhibition of stem cell-like properties of non-small cell lung carcinoma (8) and papillary thyroid carcinoma (20) cells, including generation of tumor cell spheres and the expression of stemness-related genes and proteins. In line with previous reports (8,20), the present study suggested that SHCBP1 activated CSC-related genes and promoted the self-renewal of CC cells. These findings further indicated the significance of SHCBP1 in CC.

The NF-κB signaling pathway is one of the important pathways involved in cell cycle regulation (37). NF-κB can activate the transcription of cell cycle-related genes, including cyclin D1, cyclin E1, CDK2, CDK2 and Myc, thereby modulating cell cycle distribution (38-41). The NF-κB pathway also contributes to maintaining CSC-like properties in multiple types of cancer (42-44). Overexpression of *p65* enhances the expression of CSC markers, such as CD44 and CD133, in CC cells (45). Bay-11-7082, an inhibitor of NF-κB, has been demonstrated to reduce CD44 expression in breast cancer cells (46) and NANOG and SOX2 expression in CD44-positive and myeloid differentiation primary response 88-positive ovarian

cancer cells (47). Knockdown of p65 and/or RelB decreases CD133-positive skin cancer cells, and their self-renewal abilities (48). The present study demonstrated that SHCBP1 activated the NF-κB signaling pathway in CC cells. Given the importance of NF-κB in cell proliferation and stemness maintenance in cancer cells, it is hypothesized that the pro-proliferative and pro-stemness effects of SHCBP1 may be attributed to its induction of NF-κB activation.

The positive regulation of NF-κB activation by EIF5A has been indicated in previous studies (17,19). The inhibitory effect of SHCBP1 shRNA transfection on EIF5A mRNA was confirmed in the present study. Similar effects have been observed in papillary thyroid cancer cells (20), and it was hypothesized that EIF5A may mediate the biological function of SHCBP1 and the regulation of the NF-κB signaling pathway by SHCBP1 in CC. The findings of the present study confirm this hypothesis. The regulatory mechanism of SHCBP1 on EIF5A remains unclear, which is one of the limitations of the present study. SHCBP1 could enhance the interaction between CREB-binding protein (CBP) and β-catenin, thereby activating the transcription of genes driven by β-catenin (49). The interaction between CBP and KLF5 is of importance for KLF5 transactivation activities (50). There are KLF5 binding sites at the promoter of EIF5A. KLF5 has been confirmed to bind to EIFA5 and activate its transcription (51). Based on previous studies (49-51), it was hypothesized that the regulation of EIF5A mRNA by SHCBP1 may be associated with the enhanced interaction between CBP and KLF5 triggered by SHCBP1, which needs to be explored in future work. In addition, the effect of SHCBP1 on tumor growth in a xenograft model of CC was not investigated, which may be an additional limitation of the present study.

In summary, the role of SHCBP1 in CC was identified *in vitro*. Mechanistically, SHCBP1 facilitated CC cell proliferation, stemness and activation of the NF-κB signaling pathway through EIF5A *in vitro*. The present study suggested a novel molecular mechanism underlying the progression of CC.

Availability of data and materials

The datasets used and/or analyzed during the current study are available from the corresponding author on reasonable request.

Authors' contributions

BYD conceptualized the research project, devised methodology, completed formal analysis and data curation, prepared and wrote the original draft manuscript. ALL supervised the study, performed data analysis and reviewed and edited the manuscript. YZ, YYZ and JF performed experiments and validated the data. YM performed interpretation and visualization

of the data. BYD, ALL and YM confirm the authenticity of all the raw data. All authors have read and approved the final manuscript.

Ethics approval and consent to participate

Not applicable.

Patient consent for publication

Not applicable.

Competing interests

The authors declare that they have no competing interests.

References

1. Sung H, Ferlay J, Siegel RL, Laversanne M, Soerjomataram I, Jemal A and Bray F: Global cancer statistics 2020: GLOBOCAN estimates of incidence and mortality worldwide for 36 cancers in 185 countries. CA Cancer J Clin 71: 209-249, 2021.
2. Brisson M and Drolet M: Global elimination of cervical cancer as a public health problem. Lancet Oncol 20: 319-321, 2019.
3. Brisson M, Kim JJ, Canfell K, Drolet M, Gingras G, Burger EA, Martin D, Simms KT, Bénard É, Boily MC, et al: Impact of HPV vaccination and cervical screening on cervical cancer elimination: A comparative modelling analysis in 78 low-income and lower-middle-income countries. Lancet 395: 575-590, 2020.
4. Schmandt R, Liu SK and McGlade CJ: Cloning and characterization of mPAL, a novel Shc SH2 domain-binding protein expressed in proliferating cells. Oncogene 18: 1867-1879, 1999.
5. Li D, Peng H, Qu L, Sommar P, Wang A, Chu T, Li X, Bi X, Liu Q, Sérézal IG, et al: MiR-19a/b and miR-20a promote wound healing by regulating the inflammatory response of keratinocytes. J Invest Dermatol 141: 659-671, 2021.
6. Shi W, Zhang G, Ma Z, Li L, Liu M, Qin L, Yu Z, Zhao L, Liu Y, Zhang X, et al: Hyperactivation of HER2-SHCBP1-PLK1 axis promotes tumor cell mitosis and impairs trastuzumab sensitivity to gastric cancer. Nat Commun 12: 2812, 2021.
7. Peng C, Zhao H, Song Y, Chen W, Wang X, Liu X, Zhang C, Zhao J, Li J, Cheng G, et al: SHCBP1 promotes synovial sarcoma cell metastasis via targeting TGF-beta1/Smad signaling pathway and is associated with poor prognosis. J Exp Clin Cancer Res 36: 141, 2017.
8. Liu L, Yang Y, Liu S, Tao T, Cai J, Wu J, Guan H, Zhu X, He Z, Li J, et al: EGF-induced nuclear localization of SHCBP1 activates beta-catenin signaling and promotes cancer progression. Oncogene 38: 747-764, 2019.
9. Wullaert A, Bonnet MC and Pasparakis M: NF-κB in the regulation of epithelial homeostasis and inflammation. Cell Res 21: 146-158, 2011.
10. Ghosh S and Hayden MS: New regulators of NF-kappaB in inflammation. Nat Rev Immunol 8: 837-848, 2008.
11. Wu Z, Peng X, Li J, Zhang Y and Hu L: Constitutive activation of nuclear factor kappaB contributes to cystic fibrosis transmembrane conductance regulator expression and promotes human cervical cancer progression and poor prognosis. Int J Gynecol Cancer 23: 906-915, 2013.
12. Wang J, Ou J, Guo Y, Dai T, Li X, Liu J, Xia M, Liu L and He M: TBLR1 is a novel prognostic marker and promotes epithelial-mesenchymal transition in cervical cancer. Br J Cancer 111: 112-124, 2014.
13. Wang W, Li X, Xu Y, Guo W, Yu H, Zhang L, Wang Y and Chen X: Acetylation-stabilized chloride intracellular channel 1 exerts a tumor-promoting effect on cervical cancer cells by activating NF-kappaB. Cell Oncol (Dordr) 44: 557-568, 2021.
14. Zhou Y, Tan Z, Chen K, Wu W, Zhu J, Wu G, Cao L, Zhang X, Zeng X, Li J and Zhang W: Overexpression of SHCBP1 promotes migration and invasion in gliomas by activating the NF-kappaB signaling pathway. Mol Carcinog 57: 1181-1190, 2018.
15. Coni S, Serrao SM, Yurtsever ZN, Magno LD, Bordone R, Bertani C, Licursi V, Ianniello Z, Infante P, Moretti M, et al: Blockade of EIF5A hypusination limits colorectal cancer growth by inhibiting MYC elongation. Cell Death Dis 11: 1045, 2020.
16. Wang Z, Jiang J, Qin T, Xiao Y and Han L: EIF5A regulates proliferation and chemoresistance in pancreatic cancer through the sHH signalling pathway. J Cell Mol Med 23: 2678-2688, 2019.
17. Mémin E, Hoque M, Jain MR, Heller DS, Li H, Cracchiolo B, Hanauske-Abel HM, Pe'ery T and Mathews MB: Blocking eIF5A modification in cervical cancer cells alters the expression of cancer-related genes and suppresses cell proliferation. Cancer Res 74: 552-562, 2014.
18. Liu Z, Teng L, Gao L, Wang H, Su Y and Li J: The role of eukaryotic translation initiation factor 5A-1 (eIF5A-1) gene in HPV 16 E6 induces cell growth in human cervical squamous carcinoma cells. Biochem Biophys Res Commun 504: 6-12, 2018.
19. Taylor CA, Liu Z, Tang TC, Zheng Q, Francis S, Wang TW, Ye B, Lust JA, Dondero R and Thompson JE: Modulation of eIF5A expression using SNS01 nanoparticles inhibits NF-κB activity and tumor growth in murine models of multiple myeloma. Mol Ther 20: 1305-1314, 2012.
20. Geng H, Guo M, Xu W, Zang X, Wu T, Teng F, Wang Y, Liu X, Wang X, Sun Q and Liang J: SHCBP1 promotes papillary thyroid carcinoma carcinogenesis and progression through promoting formation of integrin and collagen and maintaining cell stemness. Front Endocrinol (Lausanne) 11: 613879, 2021.
21. Scotto L, Narayan G, Nandula SV, Arias-Pulido H, Subramaniyam S, Schneider A, Kaufmann AM, Wright JD, Pothuri B, Mansukhani M and Murty VV: Identification of copy number gain and overexpressed genes on chromosome arm 20q by an integrative genomic approach in cervical cancer: Potential role in progression. Genes Chromosomes Cancer 47: 755-765, 2008.
22. den Boon JA, Pyeon D, Wang SS, Horswill M, Schiffman M, Sherman M, Zuna RE, Wang Z, Hewitt SM, Pearson R, et al: Molecular transitions from papillomavirus infection to cervical precancer and cancer: Role of stromal estrogen receptor signaling. Proc Natl Acad Sci USA 112: E3255-E3264, 2015.
23. Zhai Y, Kuick R, Nan B, Ota I, Weiss SJ, Trimble CL, Fearon ER and Cho KR: Gene expression analysis of preinvasive and invasive cervical squamous cell carcinomas identifies HOXC10 as a key mediator of invasion. Cancer Res 67: 10163-10172, 2007.
24. Livak KJ and Schmittgen TD: Analysis of relative gene expression data using real-time quantitative PCR and the 2(-Delta Delta C(T)) method. Methods 25: 402-408, 2001.
25. Mirzaei S, Saghari S, Bassiri F, Raesi R, Zarrabi A, Hushmandi K, Sethi G and Tergaonkar V: NF-κB as a regulator of cancer metastasis and therapy response: A focus on epithelial-mesenchymal transition. J Cell Physiol 237: 2770-2795, 2022.
26. Strnadel J, Choi S, Fujimura K, Wang H, Zhang W, Wyse M, Wright T, Gross E, Peinado C, Park HW, et al: eIF5A-PEAK1 signaling regulates YAP1/TAZ protein expression and pancreatic cancer cell growth. Cancer Res 77: 1997-2007, 2017.
27. Tian M, Neil JR and Schiemann WP: Transforming growth factor-β and the hallmarks of cancer. Cell Signal 23: 951-962, 2021.
28. Bertoli C, Skotheim JM and de Bruin RA: Control of cell cycle transcription during G1 and S phases. Nat Rev Mol Cell Biol 14: 518-528, 2013.
29. Mo M, Tong S, Yin H, Jin Z, Zu X and Hu X: SHCBP1 regulates STAT3/c-Myc signaling activation to promote tumor progression in penile cancer. Am J Cancer Res 10: 3138-3156, 2020.
30. Yang C, Hu JF, Zhan Q, Wang ZW, Li G, Pan JJ, Huang L, Liao CY, Huang Y, Tian YF, et al: SHCBP1 interacting with EOGT enhances O-GlcNAcylation of NOTCH1 and promotes the development of pancreatic cancer. Genomics 113: 827-842, 2021.
31. Xu N, Wu YP, Yin HB, Chen SH, Li XD, Xue XY and Gou X: SHCBP1 promotes tumor cell proliferation, migration, and invasion, and is associated with poor prostate cancer prognosis. J Cancer Res Clin Oncol 146: 1953-1969, 2020.
32. Feng W, Li HC, Xu K, Chen YF, Pan LY, Mei Y, Cai H, Jiang YM, Chen T and Feng DX: SHCBP1 is over-expressed in breast cancer and is important in the proliferation and apoptosis of the human malignant breast cancer cell line. Gene 587: 91-97, 2016.
33. Batlle E and Clevers H: Cancer stem cells revisited. Nat Med 23: 1124-1134, 2017.
34. Tyagi A, Vishnoi K, Mahata S, Verma G, Srivastava Y, Masaldan S, Roy BG, Bharti AC and Das BC: Cervical cancer stem cells selectively overexpress HPV oncoprotein E6 that controls stemness and self-renewal through upregulation of HES1. Clin Cancer Res 22: 4170-4184, 2016.

35. Feng Q, Li S, Ma HM, Yang WT and Zheng PS: LGR6 activates the Wnt/beta-catenin signaling pathway and forms a β-catenin/TCF7L2/LGR6 feedback loop in LGR6(high) cervical cancer stem cells. Oncogene 40: 6103-6114, 2021.
36. Low HY, Lee YC, Lee YJ, Wang HL, Chen YI, Chien PJ, Li ST and Chang WW: Reciprocal regulation between indoleamine 2,3-dioxigenase 1 and notch1 involved in radiation response of cervical cancer stem cells. Cancers (Basel) 12: 1547, 2020.
37. Ledoux AC and Perkins ND: NF-κB and the cell cycle. Biochem Soc Trans 42: 76-81, 2014.
38. Guttridge DC, Albanese C, Reuther JY, Pestell RG and Baldwin AS Jr: NF-kappaB controls cell growth and differentiation through transcriptional regulation of cyclin D1. Mol Cell Biol 19: 5785-5799, 1999.
39. Cheng SH, Hsia C, Leone G and Liou HC: Cyclin E and Bcl-x(L) cooperatively induce cell cycle progression in c-Rel(-/-) B cells. Oncogene 22: 8472-8486, 2003.
40. Zhu SM, Al-Mathkour M, Cao L, Khalafi S, ChenZ, Poveda J, Peng D, Lu H, Soutto M, Hu T, *et al*: CDK1 bridges NF-κB and β-catenin signaling in response to H. pylori infection in gastric tumorigenesis. Cell Rep 42: 112005, 2023.
41. Liu JL, Ma HP, Lu XL, Sun SH, Guo X and Li FC: NF-κB induces abnormal centrosome amplification by upregulation of CDK2 in laryngeal squamous cell cancer. Int J Oncol 39: 915-924, 2011.
42. Marquardt JU, Gomez-Quiroz L, Camacho LO, Pinna F, Lee YH, Kitade M, Domínguez MP, Castven D, Breuhahn K, Conner EA, *et al*: Curcumin effectively inhibits oncogenic NF-κB signaling and restrains stemness features in liver cancer. J Hepatol 63: 661-669, 2015.
43. Zhang M, Wang L, Yue Y, Zhang L, Liu T, Jing M, Liang X, Ma M, Xu S, Wang K, *et al*: ITPR3 facilitates tumor growth, metastasis and stemness by inducing the NF-κB/CD44 pathway in urinary bladder carcinoma. J Exp Clin Canc Res 40: 65, 2021.
44. Gonzalez-Torres C, Gaytan-Cervantes J, Mandujano-Tinoco EA, Ceballos-Cancino G, Garcia-Venzor A, Zampedri C, Sanchez-Maldonado P, Mojica-Espinosa R, Jimenez-Hernandez LE and Maldonado V: NF-κB participates in the stem cell phenotype of ovarian cancer cells. Arch Med Res 48: 343-351, 2017.
45. Dong W, Sun S, Cao X, Cui Y, Chen A, Li X, Zhang J, Cao J and Wang Y: Exposure to TNFalpha combined with TGFbeta induces carcinogenesis in vitro via NF-kappaB/Twist axis. Oncol Rep 37: 1873-1882, 2017.
46. Smith SM, Lyu YL and Cai L: NF-κB affects proliferation and invasiveness of breast cancer cells by regulating CD44 expression. PLoS One 9: e106966, 2014.
47. Chefetz I, Alvero AB, Holmberg JC, Lebowitz N, Craveiro V, Yang-Hartwich Y, Yin G, Squillace L, Soteras MG, Aldo P and Mor G: TLR2 enhances ovarian cancer stem cell self-renewal and promotes tumor repair and recurrence. Cell Cycle 12: 511-521, 2013.
48. Quan XX, Hawk NV, Chen W, Coupar J, Lee SK, Petersen DW, Meltzer PS, Montemarano A, Braun M, Chen Z and Van Waes C: Targeting Notch1 and IKKalpha enhanced NF-kappaB activation in CD133(+) skin cancer stem cells. Mol Cancer Ther 17: 2034-2048, 2018.
49. Sun Y, Pan H, He Y, Hu C and Gu Y: Functional roles of the SHCBP1 and KIF23 interaction in modulating the cell-cycle and cisplatin resistance of head and neck squamous cell carcinoma. Head Neck 44: 591-605, 2022.
50. Zhang Z and Teng CT: Phosphorylation of Kruppel-like factor 5 (KLF5/IKLF) at the CBP interaction region enhances its transactivation function. Nucleic Acids Res 31: 2196-2208, 2003.
51. Ma D, Zheng B, Liu HL, Zhao YB, Liu X, Zhang XH, Li Q, Shi WB, Suzuki T and Wen JK: Klf5 down-regulation induces vascular senescence through eIF5a depletion and mitochondrial fission. PLoS Biol 18: e3000808, 2020.